SIAM J. NUMER. ANAL.
Vol. 36, No. 3, pp. 935–952

EXPLICIT FINITE ELEMENT METHODS FOR SYMMETRIC HYPERBOLIC EQUATIONS*

RICHARD S. FALK† AND GERARD R. RICHTER‡

Abstract. A family of explicit space-time finite element methods for the initial boundary value problem for linear, symmetric hyperbolic systems of equations is described and analyzed. The method generalizes the discontinuous Galerkin method and, as is typical for this method, obtains error estimates of order $O(h^{n+1/2})$ for approximations by polynomials of degree $\leq n$.

Key words. finite elements, symmetric hyperbolic, explicit

AMS subject classifications. 65M60, 65M15

PII. S0036142997329463

1. Introduction.

In this paper we consider the approximate solution of linear, symmetric hyperbolic systems of equations

$$\mathcal{L}\boldsymbol{u} \equiv \boldsymbol{u}_t + \sum_{i=1}^{N} A_i \boldsymbol{u}_{x_i} + B\boldsymbol{u} = \boldsymbol{f} \quad \text{in } \Omega_T \equiv \Omega \times [0,T], \tag{1.1}$$

where $\boldsymbol{u}$ is an m-vector, $A_1, \ldots, A_N$ are symmetric $(m \times m)$ matrices, and Ω is a bounded polyhedral domain in $\mathbb{R}^N$ with boundary $\Gamma(\Omega)$. We supplement (1.1) with initial and boundary conditions of the form

$$\boldsymbol{u} = \boldsymbol{g} \qquad \text{at } t = 0, \qquad (D - \mathcal{N})\boldsymbol{u} = 0 \qquad \text{on } \Gamma(\Omega) \times [0,T], \tag{1.2}$$

where $D = \sum_{i=1}^{N} n_i A_i$, $\boldsymbol{n} = (\boldsymbol{n}_x, n_t) = (n_1, \ldots, n_N, n_t)$ is the unit outer normal in the space-time domain, and $\mathcal{N}$ is assumed to satisfy

$$\mathcal{N} + \mathcal{N}^* \geq 0. \tag{1.3}$$

Friedrichs [2] has shown that (1.1)–(1.2) has a unique solution under appropriate smoothness conditions and the additional assumptions

$$B + B^* - \sum_{i=1}^{N} \frac{\partial A_i}{\partial x_i} \geq \sigma I, \ \ \sigma > 0,$$
$$\ker(D - \mathcal{N}) + \ker(D + \mathcal{N}) = \mathbb{R}^m \text{ on } \Gamma(\Omega) \times [0,T].$$

To obtain results about our numerical approximation scheme, we shall assume that (1.1)–(1.2) has a unique solution and that the slightly weaker hypothesis

$$B + B^* - \sum_{i=1}^{N} \frac{\partial A_i}{\partial x_i} \geq 0 \tag{1.4}$$

*Received by the editors November 3, 1997; accepted for publication (in revised form) May 4, 1998; published electronically May 5, 1999. The authors were supported in part by NSF grant DMS-9704556 and DARPA grant 4-23685, respectively.
http://www.siam.org/journals/sinum/36-3/32946.html
†Department of Mathematics, Rutgers University, Piscataway, NJ 08854 (falk@math.rutgers.edu).
‡Department of Computer Science, Rutgers University, Piscataway, NJ 08854 (richter@cs.rutgers.edu).

is satisfied. Two systems of this form which have important physical applications are the following.

Example 1. The damped wave equation, $\Omega \subset \mathbb{R}^2$:

$$\begin{aligned} &w_{tt} + \beta w_t - w_{xx} - w_{yy} = \phi, \ \ \beta \geq 0, \\ &w, w_t \text{ given at } t = 0, \\ &w = 0 \text{ on } \Gamma(\Omega). \end{aligned}$$

Defining $u_1 = w_x, u_2 = w_y, u_3 = w_t$, we have

$$\boldsymbol{u}_t + \begin{pmatrix} 0 & 0 & -1 \\ 0 & 0 & 0 \\ -1 & 0 & 0 \end{pmatrix} \boldsymbol{u}_x + \begin{pmatrix} 0 & 0 & 0 \\ 0 & 0 & -1 \\ 0 & -1 & 0 \end{pmatrix} \boldsymbol{u}_y + \begin{pmatrix} 0 & 0 & 0 \\ 0 & 0 & 0 \\ 0 & 0 & \beta \end{pmatrix} \boldsymbol{u} = \begin{pmatrix} 0 \\ 0 \\ \phi \end{pmatrix}.$$

Here

$$D = \begin{pmatrix} 0 & 0 & -n_1 \\ 0 & 0 & -n_2 \\ -n_1 & -n_2 & 0 \end{pmatrix}.$$

The choice

$$\mathcal{N} = \begin{pmatrix} 0 & 0 & n_1 \\ 0 & 0 & n_2 \\ -n_1 & -n_2 & 2 \end{pmatrix}$$

gives

$$D - \mathcal{N} = 2 \begin{pmatrix} 0 & 0 & -n_1 \\ 0 & 0 & -n_2 \\ 0 & 0 & -1 \end{pmatrix}, \qquad D + \mathcal{N} = 2 \begin{pmatrix} 0 & 0 & 0 \\ 0 & 0 & 0 \\ -n_1 & -n_2 & 1 \end{pmatrix},$$

$$\mathcal{N} + \mathcal{N}^* = \begin{pmatrix} 0 & 0 & 0 \\ 0 & 0 & 0 \\ 0 & 0 & 4 \end{pmatrix}.$$

Example 2. Maxwell's equations, $\Omega \subset \mathbb{R}^3$. Although these equations are of slightly more general form than (1.1), the methods and analysis presented in this paper can be easily extended to cover them.

$$\begin{aligned} &\begin{pmatrix} \epsilon I & 0 \\ 0 & \mu I \end{pmatrix} \frac{\partial}{\partial t} \begin{pmatrix} \boldsymbol{E} \\ \boldsymbol{H} \end{pmatrix} + \bigtriangledown \times \begin{pmatrix} -\boldsymbol{H} \\ \boldsymbol{E} \end{pmatrix} + \begin{pmatrix} \sigma & 0 \\ 0 & 0 \end{pmatrix} \begin{pmatrix} \boldsymbol{E} \\ \boldsymbol{H} \end{pmatrix} = \begin{pmatrix} \boldsymbol{J} \\ 0 \end{pmatrix}, \\ &\boldsymbol{E}, \boldsymbol{H} \ \text{ given at } t = 0, \qquad \boldsymbol{E} \times (n_1, n_2, n_3) = 0 \ \text{ on } \Gamma(\Omega) \times [0, T]. \end{aligned}$$

Taking $\boldsymbol{u} = \begin{pmatrix} \boldsymbol{E} \\ \boldsymbol{H} \end{pmatrix}$, we have

$$\begin{pmatrix} \epsilon I & 0 \\ 0 & \mu I \end{pmatrix} \boldsymbol{u}_t + \begin{pmatrix} 0 & M_{23} \\ M_{23}^* & 0 \end{pmatrix} \boldsymbol{u}_{x_1} + \begin{pmatrix} 0 & M_{31} \\ M_{31}^* & 0 \end{pmatrix} \boldsymbol{u}_{x_2} + \begin{pmatrix} 0 & M_{12} \\ M_{12}^* & 0 \end{pmatrix} \boldsymbol{u}_{x_3} + \begin{pmatrix} \sigma & 0 \\ 0 & 0 \end{pmatrix} \boldsymbol{u} = \begin{pmatrix} \boldsymbol{J} \\ 0 \end{pmatrix},$$

where M_{kl} is a 3×3 matrix with elements

$$(M_{kl})_{ij} = \begin{cases} 1 & \text{if } i = k, j = l, \\ -1 & \text{if } i = l, j = k, \\ 0 & \text{otherwise.} \end{cases}$$

In this case,

$$D = \begin{pmatrix} 0 & Z \\ Z^* & 0 \end{pmatrix}, \text{ where } Z = \begin{pmatrix} 0 & n_3 & -n_2 \\ -n_3 & 0 & n_1 \\ n_2 & -n_1 & 0 \end{pmatrix}.$$

The choice

$$\mathcal{N} = \begin{pmatrix} Z & Z \\ Z & 0 \end{pmatrix}$$

gives

$$D - \mathcal{N} = -\begin{pmatrix} Z & 0 \\ 2Z & 0 \end{pmatrix}, \qquad D + \mathcal{N} = \begin{pmatrix} Z & 2Z \\ 0 & 0 \end{pmatrix}, \qquad \mathcal{N} + \mathcal{N}^* = \begin{pmatrix} 0 & 0 \\ 0 & 0 \end{pmatrix}.$$

For the problem (1.1)–(1.2), we introduce a finite element scheme using elements in the space-time domain Ω_T. The method is explicit in time, easily parallelizable, and readily amenable to local mesh refinement. Our basic approach is a generalization of the discontinuous Galerkin method, introduced in [9] and studied by many authors (e.g., [4], [5], [10], [11], [12]). While space-time finite element methods for the problem (1.1)–(1.2) and more general positive symmetric systems have been proposed previously (e.g., see [4], [8], and [13]), none of these methods are explicit in time with the exception of [13], which is restricted to one space dimension. A method proposed in [4], for example, uses the discontinuous Galerkin method to break the problem into a sequence of problems on time slabs $\Omega \times [t_n, t_{n+1}]$. Within each time slab, however, the method is implicit. Other methods for this problem use finite elements to discretize in space, but the time discretization is done using finite difference or other time discretization methods. Examples of such methods can be found in [1], [3], [6], and [7].

We now describe our finite element method. We divide the space-time domain into a mesh of elements K which are unions of simplices in $\mathbb{R}^{N+1}$. Let $\Gamma^*(K)$ denote the intersection (if any) of $\Gamma(K)$ (the boundary of K) with $\Gamma(\Omega) \times [0, T]$. On $\Gamma(K) - \Gamma^*(K)$, we require $n_t \neq 0$ and define

$$\mathcal{M} \equiv \text{sign}\{n_t\}\ (n_t I + D).$$

For a function $\boldsymbol{v}$ which is discontinuous on the interface between adjoining elements K and K', we define one-sided limits $\boldsymbol{v}^{\pm}(P) = \lim_{\epsilon \to 0+} \boldsymbol{v}(P \pm \epsilon \hat{t})$, where $\hat{t}$ is a unit vector oriented in the positive t direction, and use the notation $[\boldsymbol{v}] = \boldsymbol{v}^+ - \boldsymbol{v}^-$. We then define the bilinear form

$$a(\boldsymbol{u}, \boldsymbol{v}) \equiv (\mathcal{L}\boldsymbol{u}, \boldsymbol{v})_K + \int_{\Gamma_{\text{in}}(K)} [\mathcal{M}\boldsymbol{u}] \cdot \boldsymbol{v} + \frac{1}{2} \int_{\Gamma^*(K)} (\mathcal{N} - D)\boldsymbol{u} \cdot \boldsymbol{v},$$

where, in general, $(\ ,\ )$ denotes an L^2 inner product over the indicated domain and $\Gamma_{\text{in}}(K)$ ($\Gamma_{\text{out}}(K)$) denotes the portion of $\Gamma(K) - \Gamma^*(K)$, where $n_t < 0$ ($n_t > 0$).

A key mesh condition required by our method is that the solution to (1.1) within each element K be uniquely determined by $\boldsymbol{u}$ on $\Gamma_{\text{in}}(K)$ and the boundary condition on $\Gamma^*(K)$ given in (1.2) in the case where $\Gamma^*(K)$ is nonempty. The mesh will then be traversable in an explicit, element-by-element fashion, in the direction of increasing t, without violating any domain of dependence conditions. The finite element approximation is developed in the same way. Mathematical conditions guaranteeing explicitness of the mesh are given in the next section.

On each element K, we shall approximate $\boldsymbol{u}$ by $\boldsymbol{u}_h \in \boldsymbol{P}_n(K)$, where $\boldsymbol{P}_n(K)$ consists of polynomials of degree $\leq n$ over K. Our finite element approximation $\boldsymbol{u}_h$ starts as an appropriate interpolant $\boldsymbol{u}_h^-(\boldsymbol{x}, 0)$ of the given initial condition and is developed in individual elements K by

$$a(\boldsymbol{u}_h, \boldsymbol{v}_h) = (\boldsymbol{f}, \boldsymbol{v}_h)_K \qquad \text{for all } \boldsymbol{v}_h \in \boldsymbol{P}_n(K). \tag{1.5}$$

In our analysis, we make the usual assumptions of mesh quasi uniformity (the ratio of radii of the smallest circumscribing spheres of any two elements must be bounded) and nondegeneracy (the ratio of the smallest circumscribing sphere to the largest inscribing sphere of any element K must be bounded independent of K). An additional property, which we need for a local stability result, is that each element K is convex or has a total number of inflow and outflow faces exceeding n, the degree of the polynomial approximate solution within K. This technical assumption will also become clearer when we describe the construction of a mesh satisfying these conditions in section 2.

The main result of the paper will be to prove that with a mesh constructed to satisfy the above hypotheses, the method produces a piecewise polynomial approximation $\boldsymbol{u}_h$ to $\boldsymbol{u}$ which satisfies

$$|\boldsymbol{u} - \boldsymbol{u}_h^-|^2_{\Gamma_{\text{out}}(\Omega_T)} + \sum_{K \subset \Omega_T} |[\boldsymbol{u} - \boldsymbol{u}_h]|^2_{\Gamma_{\text{in}}(K)} + \|\boldsymbol{u} - \boldsymbol{u}_h\|^2_{\Omega_T} \leq C(\boldsymbol{u}) h^{2n+1},$$

where $\|\cdot\|_{k,\Omega}$ denotes the norm on $H^k(\Omega)$, with k omitted when it has value zero and a "surface" L^2 norm over $\Gamma(K)$ is denoted by $|\cdot|$. Details of the dependence of $C(\boldsymbol{u})$ on specific norms of $\boldsymbol{u}$ may be found in section 4.

An outline of the paper is as follows: In the next section we describe in detail the construction of a finite element mesh which satisfies the properties given above. A stability estimate for the finite element scheme is derived in section 3 and error estimates are obtained in section 4. Finally, some computational results are presented in section 5.

2. Mesh construction and properties. As mentioned in the introduction, we propose to divide the space-time domain into elements K which are unions of simplices in $\mathbb{R}^{N+1}$ and have the property that they are "explicitly" configured with respect to domain of dependence. To understand what this means, first consider the homogeneous equation

$$\mathcal{L}\boldsymbol{u} = \boldsymbol{u}_t + \sum_{i=1}^{N} A_i \boldsymbol{u}_{x_i} + B\boldsymbol{u} = 0.$$

Integrating against $\boldsymbol{u}$ over K, we get

$$\frac{1}{2}\int_{\Gamma(K)} (n_t + D)\boldsymbol{u} \cdot \boldsymbol{u} + \int_K \left[B - \frac{1}{2}\sum_{i=1}^{N} \frac{\partial A_i}{\partial x_i} \right] \boldsymbol{u} \cdot \boldsymbol{u} = 0. \tag{2.1}$$

We may rewrite (2.1) as

$$\int_{\Gamma_{\text{out}}(K)} (\mathcal{M}\boldsymbol{u})\cdot\boldsymbol{u} + \int_{\Gamma^*(K)} D\boldsymbol{u}\cdot\boldsymbol{u} = \int_{\Gamma_{\text{in}}(K)} (\mathcal{M}\boldsymbol{u})\cdot\boldsymbol{u} - \int_K \left[B + B^* - \sum_{i=1}^N \frac{\partial A_i}{\partial x_i}\right]\boldsymbol{u}\cdot\boldsymbol{u}.$$

On $\Gamma^*(K)$, $D\boldsymbol{u}\cdot\boldsymbol{u} = \mathcal{N}\boldsymbol{u}\cdot\boldsymbol{u} \geq 0$ via (1.2) and (1.3). Thus, assuming 1.4, we obtain

$$\int_{\Gamma_{\text{out}}(K)} \mathcal{M}\boldsymbol{u}\cdot\boldsymbol{u} \leq \int_{\Gamma_{\text{in}}(K)} \mathcal{M}\boldsymbol{u}\cdot\boldsymbol{u}.$$

We require the eigenvalues λ of $\mathcal{M}$ to satisfy a uniform bound:

$$0 < \gamma \leq \lambda(\mathcal{M}) \leq \mu. \tag{2.2}$$

Note that $\operatorname{sign}\{n_t\}\ n_t I = |n_t| I$ and that $\|D\| \leq \sqrt{N}|\boldsymbol{n}_x| \max_i \|A_i\|$, where $|\boldsymbol{n}_x|^2 = \sum_{i=1}^N n_i^2$. Satisfaction of (2.2) is therefore guaranteed if the boundary $\Gamma(K)$ is inclined sufficiently toward the $\boldsymbol{x}$-plane. In particular, if

$$\frac{|\boldsymbol{n}_x|}{|n_t|} < \frac{1}{\sqrt{N}\max_i \|A_i\|},$$

(2.2) will be satisfied. With such a construction, we have the relation for the L^2 norms of $\boldsymbol{u}$ over $\Gamma_{\text{in}}(K)$ and $\Gamma_{\text{out}}(K)$

$$|\boldsymbol{u}|^2_{\Gamma_{\text{out}}(K)} \leq \frac{\mu}{\gamma}|\boldsymbol{u}|^2_{\Gamma_{\text{in}}(K)},$$

implying that the solution on $\Gamma_{\text{out}}(K)$ is determined solely by data on $\Gamma_{\text{in}}(K)$. The same is true of the solution within K. We may therefore regard $\boldsymbol{u}$ as moving across K from $\Gamma_{\text{in}}(K)$ to $\Gamma_{\text{out}}(K)$, i.e., in the direction of increasing t. Thus, we will use the condition (2.2) to guarantee that the mesh is explicitly configured with respect to domain of dependence. A second condition, which we will require for a local stability result, is that

(2.3) each element K is convex or has a total number of inflow and outflow faces exceeding n, the degree of the polynomial approximate solution within K.

In general, our elements will be unions of simplices, and these unions may not be convex. An example illustrating this will be presented later in the section.

It is useful to represent the domain of dependence relations among elements by a directed graph. The nodes are the elements K and there is an edge from K to K' if $\Gamma_{\text{out}}(K) \cap \Gamma_{\text{in}}(K') \neq \emptyset$. Condition (2.2) ensures that this directed graph is acyclic, thus guaranteeing that it can be traversed in accordance with the precedence relations given by its edges. Equivalently, the elements can be ordered explicitly with respect to domain of dependence. In general, there would be many such orderings. It will be convenient for us to think of the solution as evolving in layers S_i defined by

$$\begin{aligned} S_1 &= \{K|\Gamma_{\text{in}}(K) \subset \Gamma_{\text{in}}(\Omega_T)\}, \\ S_i &= \left\{K|\Gamma_{\text{in}}(K) \subset \Gamma_{\text{in}}(\Omega_T) - \Gamma_{\text{in}}\left(\cup_{j<i}S_j\right) \cup \Gamma_{\text{out}}\left(\cup_{j<i}S_j\right)\right\}, \qquad i = 2,3,\ldots. \end{aligned} \tag{2.4}$$

We also denote by $\mathcal{F}_i$ the "front" to which the solution has advanced after it has evolved through $\cup_{j\leq i}S_j$. Note that the solution can be developed in parallel over the

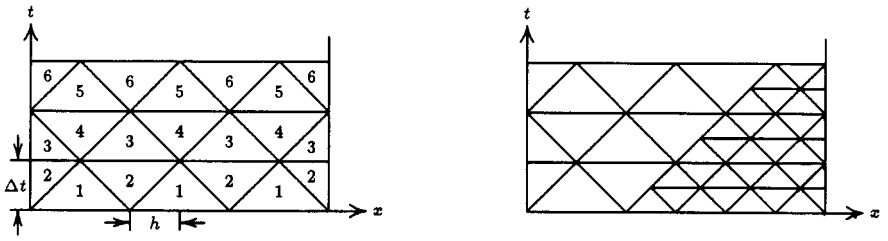

(a) (b)

FIG. 2.1.

elements within each layer. In our analysis, we assume there are $O(h^{-1})$ layers in Ω_T. Our mesh construction strategy will produce such a mesh.

As a simple illustration of these ideas, consider a wave equation problem with $\Omega \subset \mathbb{R}^1$:

$$u_{tt} - u_{xx} = f, \qquad x \in (0,1), \;\; t > 0.$$

Equivalently,

$$\boldsymbol{u}_t + \begin{pmatrix} 0 & -1 \\ -1 & 0 \end{pmatrix} \boldsymbol{u}_x = \begin{pmatrix} 0 \\ f \end{pmatrix}, \qquad \boldsymbol{u} \equiv \begin{pmatrix} u_x \\ u_t \end{pmatrix}.$$

Here $\mathcal{M} = \operatorname{sign}\{n_t\} \left(\begin{smallmatrix} n_t & -n_x \\ -n_x & n_t \end{smallmatrix} \right)$ and $\lambda(\mathcal{M}) = \operatorname{sign}\{n_t\}(n_t \pm n_x)$. Thus (2.2) will be satisfied if $|n_x| < |n_t|$ on all interelement boundaries. Two such meshes are depicted in Figure 2.1. Figure 2.1(a) shows a partition of the space-time domain into time slabs, each consisting of congruent isosceles triangles, numbered by the layers S_i to which they belong. Figure 2.1(b) illustrates the possibility of local mesh refinement (by means of a four-for-one subdivision), a potentially important capability. This contrasts with the more customary numerical approach of first semidiscretizing in space and then advancing the solution from one discrete time to the next using a time-stepping scheme. If the spatial discretization is highly nonuniform, an explicit time integration scheme may require an inordinately small time step, while use of an implicit method may yield poor resolution in the refined region. Note that a conforming mesh is not needed for our finite element method since it generates a discontinuous approximation.

By removing all horizontal interfaces in Figure 2.1, we obtain alternative meshes depicted in Figure 2.2. Here the solution would not be brought to discrete times $\{t_n\}$; however, we now have half as many elements as before and only one generic interior element: a rhombus standing on end, suitably compressed in the t-direction so as to satisfy (2.2).

We next consider the case $\Omega \subset \mathbb{R}^2$. Starting from a given triangulation of Ω, we will show how to obtain space-time elements $\{K\}$ whose surfaces (except those contained by $\Gamma(\Omega) \times [0,T]$) have outer normal $\boldsymbol{n} = (\boldsymbol{n}_x, n_t)$ satisfying

$$|\boldsymbol{n}_x|/|n_t| \le \theta \tag{2.5}$$

for arbitrary $\theta > 0$. By choosing θ small enough, the explicitness condition (2.2) will be guaranteed to hold. The mesh generation scheme we shall present is readily manageable computationally, supports the use of local mesh refinement, and is extendable to domains Ω of arbitrarily high dimension.

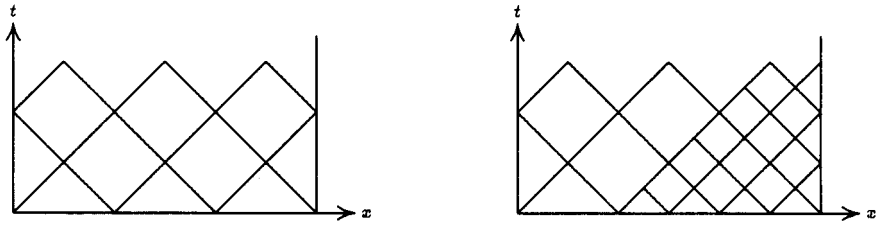

(a) (b)

FIG. 2.2.

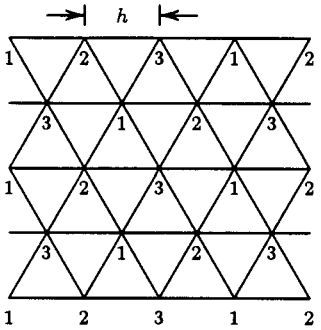

FIG. 2.3.

As our first two-space-dimensional example, we consider a domain Ω which admits a uniform equilateral triangulation, as shown in Figure 2.3, and indicate how a corresponding time slab $\Omega \times [0, \Delta t]$ can be partitioned. We denote by $\mathcal{X}$ the vertices of the triangulation and refer to $\boldsymbol{x}, \boldsymbol{x}' \in \mathcal{X}$ as neighbors, denoted by $\boldsymbol{x}' \in \mathcal{N}(\boldsymbol{x})$ (or $\boldsymbol{x} \in \mathcal{N}(\boldsymbol{x}')$), if some triangle contains both of them. In Figure 2.3, each vertex has been assigned a "color" $c(\boldsymbol{x}) \in \{1, 2, 3\}$ in such a way that $\boldsymbol{x}' \in \mathcal{N}(\boldsymbol{x}) \implies c(\boldsymbol{x}') \neq c(\boldsymbol{x})$. This coloring condition cannot be satisfied with fewer than three colors; hence the indicated coloring is minimal.

Now choose an arbitrary vertex $\boldsymbol{x}^* \in \mathcal{X}$ with $c(\boldsymbol{x}^*) = 1$. Our first (macro)element K in the space-time domain will be the convex hull of $(\boldsymbol{x}^*, 0)$, $(\boldsymbol{x}^*, \Delta t)$, and $\{(\boldsymbol{x}', 0) : \boldsymbol{x}' \in \mathcal{N}(\boldsymbol{x}^*)\}$, consisting of six tetrahedra with a common edge $(\boldsymbol{x}^*, t)$, $0 \leq t \leq \Delta t$. The outer normal to K satisfies $|\boldsymbol{n}_x|/|n_t| \leq (2/\sqrt{3})(\Delta t/h)$; thus (2.5) can be achieved by taking $\Delta t = (\sqrt{3}/2)h\theta$. This is the maximum local time step consistent with (2.5). Note that a solution can be developed simultaneously in all such elements K centered about vertices of color 1, since these are nonintersecting for $t > 0$. Thus these elements comprise S_1 as defined in (2.4). At the completion of this step, the space-time mesh will have advanced to the front $\mathcal{F}_1$, a piecewise planar surface with vertex set $V = \{(\boldsymbol{x}, t(\boldsymbol{x})) | \boldsymbol{x} \in \mathcal{X}\}$, where $t(\boldsymbol{x}) = \Delta t$ if $c(\boldsymbol{x}) = 1$ and $t(\boldsymbol{x}) = 0$ if $c(\boldsymbol{x}) \neq 1$.

In the second step, the mesh is advanced to $t = \Delta t$ at each vertex having color 2. Suppose $c(\boldsymbol{x}^*) = 2$; the corresponding element is then the convex hull of $(\boldsymbol{x}^*, 0)$, $(\boldsymbol{x}^*, \Delta t)$, $\{(\boldsymbol{x}', \Delta t) | \boldsymbol{x}' \in \mathcal{N}(\boldsymbol{x}^*), c(\boldsymbol{x}') = 1\}$, and $\{(\boldsymbol{x}', 0) | \boldsymbol{x}' \in \mathcal{N}(\boldsymbol{x}^*), c(\boldsymbol{x}') > 1\}$, again a union of 6 tetrahedra (with noncoplanar bases) having a common edge $(\boldsymbol{x}^*, t)$, $0 \leq$

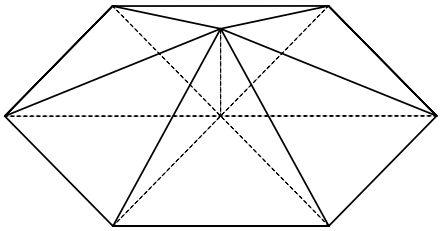

FIG. 2.4. *Macroelement of color* 1.

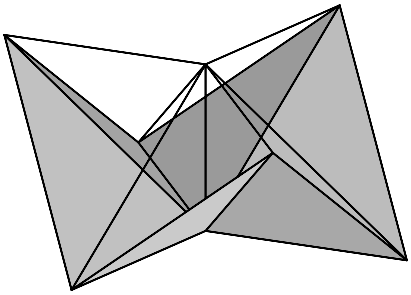

FIG. 2.5. *Macroelement of color* 2.

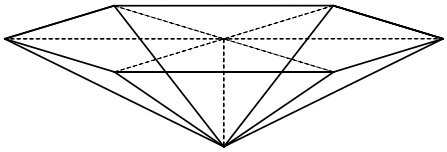

FIG. 2.6. *Macroelement of color* 3.

$t \leq \Delta t$. The maximum value of $|n_t|$ for these elements will be the same as for elements in S_1. After this step, the solution will have advanced to $\mathcal{F}_2$, with vertex set $V = \{(\boldsymbol{x}, t(\boldsymbol{x}))|\boldsymbol{x} \in \mathcal{X}\}$, where $t(\boldsymbol{x}) = \Delta t$ if $c(\boldsymbol{x}) \leq 2$ and 0 otherwise. In an analogous third step, the space-time mesh can be brought up to $t = \Delta t$ at the remaining (color 3) vertices in $\mathcal{X}$. (An alternative third step would be to raise the mesh to time $t = 2\Delta t$ at color 3 vertices with an element twice as large.) Elements for steps 1, 2, and 3, as described, all have the same volume: $(3/4)h^3\theta$; those in steps 1 and 3 are convex, while those in step 2 are nonconvex and have 12 faces. Note that to satisfy (2.3), the polynomial approximation within the nonconvex element would have to be of degree < 12. Elements of the 3 types described above are depicted in Figures 2.4, 2.5, and 2.6, respectively. In Figure 2.5, the element lies above the solid faces shown and below the faces indicated by the solid lines.

In Figure 2.7, a developing mesh is shown, just after the formation of elements of colors 1 and 2. Note that an element of color 3 is now needed to bring the mesh up to the next time level.

We now give several other examples of space-time meshes that can be derived in an analogous way from particular triangulations of the spatial domain. For the regular right isosceles triangulation shown in Figure 2.8, the corresponding graph is 3-colorable, as indicated, and each color may again be regarded as corresponding to a layer of elements as previously described. Here elements of colors 1, 2, and 3 again

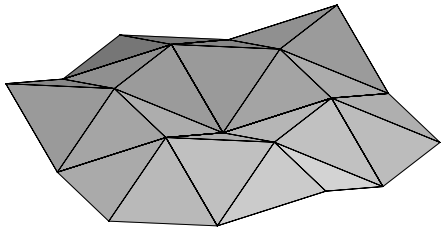

FIG. 2.7. *Developing mesh.*

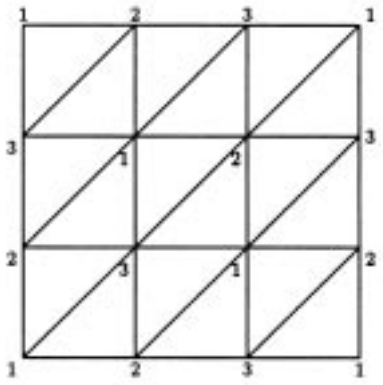

FIG. 2.8.

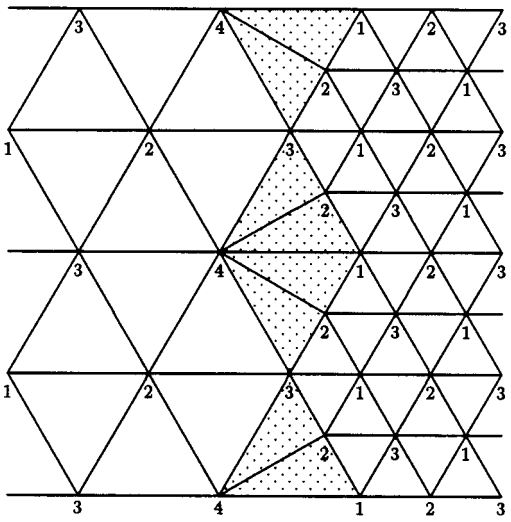

FIG. 2.9.

consist of 6, 6, and 6 tetrahedra, and (2.5) will be satisfied if $\Delta t \leq (1/\sqrt{2})h\theta$.

Figure 2.9 depicts a mesh refinement situation, with two subregions of equilateral triangles of side length h and $h/2$ and an interface between them. A (minimal) 4-coloring is given. As before, the elements in S_1 will be unions of tetrahedra centered

about vertices of color 1. These separate into three classes: those in the regular mesh on the left (which may extend to a maximum height $\Delta t = (\sqrt{3}/2)h\theta$), those to the right of the interface (having height $\Delta t/2$), and those on the interface (which consist of fewer than six tetrahedra and also have height $\Delta t/2$). The situation is similar for vertices of colors 2, 3, and 4. At the completion of the first four parallel steps, the space-time mesh will have advanced to time Δt to the left of the interface and $\Delta t/2$ to the right. An additional three steps in the latter region will bring the mesh to $t = \Delta t$ at all vertices.

The same basic mesh construction scheme can be used for the general case of an unstructured $\mathcal{X}$. Each front $\mathcal{F}_i$—as before a piecewise planar surface in $\mathbb{R}^3$—is characterized by its vertex set $V = \{(\boldsymbol{x}, t(\boldsymbol{x}))|x \in \mathcal{X}\}$. The next layer $\mathcal{S}_{i+1}$ is composed of elements K associated with particular members of $\mathcal{X}$. The element corresponding to $x^* \in \mathcal{X}$ advances the mesh to a later time at x^* but at no other $x \in \mathcal{X}$. A coloring of $\mathcal{X}$ will indicate which elements can be generated and processed concurrently. One can also add to or delete from $\mathcal{X}$ as the mesh advances in order to resolve a moving transient; this was done in the mesh of Figure 2.1(b).

We conclude this discussion with a generalization to the case $\Omega \subset \mathbb{R}^2$ of the mesh depicted in Figure 2.2(a). Returning to $t = 0$ and the spatial configuration of Figure 2.3, suppose we raise vertices of color 1 to $t = \Delta t$ in the first step and advance vertices of color 2 to $t = 2\Delta t$ in the second step. The maximum Δt consistent with (2.5) is $\Delta t = (1/2)h\theta$. If, in the third step, we raise vertices of color 3 to $t = 3\Delta t$, then the corresponding elements in this step are hexahedra, which can be visualized as the result of "balancing" a cube on one of its vertices and then compressing sufficiently in the t direction to satisfy (3.1). Moreover, in the next step, we have the analogous situation, in which vertices of color 1 are brought to $t = 4\Delta t$ with the same hexahedral elements as in the previous step, etc. This scheme produces one generic hexahedral element in contrast with three different elements for the time slab scheme. The volume of the hexahedron is $\sqrt{3}$ times that of the time slab elements, so that fewer elements would be needed to cover a given domain Ω_T. Local mesh refinement can be accomplished by a one-into-eight subdivision of elements.

3. Stability of the approximation scheme. We begin by defining

$$\mathcal{L}^*\boldsymbol{v} \equiv -\frac{\partial \boldsymbol{v}}{\partial t} - \sum_{i=1}^{N} A_i \frac{\partial \boldsymbol{v}}{\partial x_i} + \left[B^* - \sum_{i=1}^{N} \frac{\partial A_i}{\partial x_i} \right] \boldsymbol{v}.$$

Then we have the following identity.

LEMMA 3.1.

$$(3.1)\quad a(\boldsymbol{u},\boldsymbol{v}) = (\boldsymbol{u}, \mathcal{L}^*\boldsymbol{v})_K - \int_{\Gamma_{in}(K)} [\mathcal{M}\boldsymbol{v}] \cdot \boldsymbol{u} - \frac{1}{2}\int_{\Gamma^*(K)} (\mathcal{N} - D)\boldsymbol{v} \cdot \boldsymbol{u}$$
$$+ \oint_{\Gamma(K)-\Gamma^*(K)} \mathcal{M}\boldsymbol{u}^- \cdot \boldsymbol{v}^- sign\{n_t\} + \int_{\Gamma_{in}(K)} \mathcal{M}[\boldsymbol{u}] \cdot [\boldsymbol{v}] + \frac{1}{2}\int_{\Gamma^*(K)} (\mathcal{N} + \mathcal{N}^*)\boldsymbol{u} \cdot \boldsymbol{v}.$$

Proof. Integrating by parts, we obtain

$$a(\boldsymbol{u},\boldsymbol{v}) = (\boldsymbol{u}, \mathcal{L}^*\boldsymbol{v})_K + \int_{\Gamma_{\text{out}}(K)} \mathcal{M}\boldsymbol{u}^- \cdot \boldsymbol{v}^- - \int_{\Gamma_{\text{in}}(K)} \mathcal{M}\boldsymbol{u}^+ \cdot \boldsymbol{v}^+$$
$$+ \int_{\Gamma_{\text{in}}(K)} [\mathcal{M}\boldsymbol{u}] \cdot \boldsymbol{v}^+ + \frac{1}{2}\int_{\Gamma^*(K)} (\mathcal{N} + D)\boldsymbol{u} \cdot \boldsymbol{v}.$$

The integrand along $\Gamma_{\text{in}}(K)$ can be written

$$\begin{aligned}-\mathcal{M}\boldsymbol{u}^+\cdot\boldsymbol{v}^+ + [\mathcal{M}\boldsymbol{u}]\cdot\boldsymbol{v}^+ &= -\mathcal{M}\boldsymbol{u}^-\cdot\boldsymbol{v}^+\\ &= -\mathcal{M}\boldsymbol{u}^-\cdot(\boldsymbol{v}^- + [\boldsymbol{v}])\\ &= -\mathcal{M}\boldsymbol{u}^-\cdot\boldsymbol{v}^- - \mathcal{M}(\boldsymbol{u}^+ - [\boldsymbol{u}])\cdot[\boldsymbol{v}]\\ &= -\mathcal{M}\boldsymbol{u}^-\cdot\boldsymbol{v}^- - \mathcal{M}\boldsymbol{u}^+\cdot[\boldsymbol{v}] + \mathcal{M}[\boldsymbol{u}]\cdot[\boldsymbol{v}]\\ &= -\mathcal{M}\boldsymbol{u}^-\cdot\boldsymbol{v}^- - [\mathcal{M}\boldsymbol{v}]\cdot\boldsymbol{u}^+ + \mathcal{M}[\boldsymbol{u}]\cdot[\boldsymbol{v}].\end{aligned}$$

In addition, along $\Gamma^*(K)$,

$$(\mathcal{N}+D)\boldsymbol{u}\cdot\boldsymbol{v} = -(\mathcal{N}-D)\boldsymbol{v}\cdot\boldsymbol{u} + (\mathcal{N}+\mathcal{N}^*)\boldsymbol{u}\cdot\boldsymbol{v}.$$

Hence

$$\begin{aligned}a(\boldsymbol{u},\boldsymbol{v}) = (\mathcal{L}^*\boldsymbol{v},\boldsymbol{u})_K - \int_{\Gamma_{\text{in}}(K)}[\mathcal{M}\boldsymbol{v}]\cdot\boldsymbol{u}^+ - \frac{1}{2}\int_{\Gamma^*(K)}(\mathcal{N}-D)\boldsymbol{v}\cdot\boldsymbol{u} + \int_{\Gamma_{\text{out}}(K)}\mathcal{M}\boldsymbol{u}^-\cdot\boldsymbol{v}^-\\ - \int_{\Gamma_{\text{in}}(K)}\mathcal{M}\boldsymbol{u}^-\cdot\boldsymbol{v}^- + \int_{\Gamma_{\text{in}}(K)}\mathcal{M}[\boldsymbol{u}]\cdot[\boldsymbol{v}] + \frac{1}{2}\int_{\Gamma^*(K)}(\mathcal{N}+\mathcal{N}^*)\boldsymbol{u}\cdot\boldsymbol{v},\end{aligned}$$

which proves the result. □

It follows immediately from (3.1) that

(3.2)

$$\begin{aligned}a(\boldsymbol{u},\boldsymbol{u}) &= \frac{1}{2}\left(\left[B + B^* - \sum_{i=1}^{N}\frac{\partial A_i}{\partial x_i}\right]\boldsymbol{u},\boldsymbol{u}\right)_K + \frac{1}{2}\oint_{\Gamma(K)-\Gamma^*(K)}\mathcal{M}\boldsymbol{u}^-\cdot\boldsymbol{u}^-\operatorname{sign}\{n_t\}\\ &\quad + \frac{1}{2}\int_{\Gamma_{\text{in}}(K)}\mathcal{M}[\boldsymbol{u}]\cdot[\boldsymbol{u}] + \frac{1}{4}\int_{\Gamma^*(K)}(\mathcal{N}+\mathcal{N}^*)\boldsymbol{u}\cdot\boldsymbol{u}\\ &\geq \frac{1}{2}\oint_{\Gamma(K)-\Gamma^*(K)}\mathcal{M}\boldsymbol{u}^-\cdot\boldsymbol{u}^-\operatorname{sign}\{n_t\} + \frac{\gamma}{2}|[\boldsymbol{u}]|^2_{\Gamma_{\text{in}}(K)} + \frac{1}{4}\int_{\Gamma^*(K)}(\mathcal{N}+\mathcal{N}^*)\boldsymbol{u}\cdot\boldsymbol{u}.\end{aligned}$$

LEMMA 3.2. *$\boldsymbol{u}_h$ is well defined in K and satisfies, for h sufficiently small, the local bound*

$$\|\boldsymbol{u}_h\|_K \leq C\left(\sqrt{h}|\boldsymbol{u}_h^-|_{\Gamma_{in}(K)} + h\|f\|_K\right). \tag{3.3}$$

Proof. Scaling the inner product conditions (1.5) to an element $\hat{K}$ with diameter one, we get

$$\begin{aligned}&\left((\hat{\boldsymbol{u}}_h)_{\hat{t}} + \sum_{i=1}^{N}\hat{A}_i(\hat{\boldsymbol{u}}_h)_{\hat{x}_i} + h\hat{B}\hat{\boldsymbol{u}}_h,\hat{\boldsymbol{v}}_h\right)_{\hat{K}} + \int_{\Gamma_{\text{in}}(\hat{K})}\hat{\mathcal{M}}\hat{\boldsymbol{u}}_h^+\cdot\hat{\boldsymbol{v}}_h\\ &\qquad + \frac{1}{2}\int_{\Gamma^*(\hat{K})}(\hat{\mathcal{N}}-\hat{D})\hat{\boldsymbol{u}}_h\cdot\hat{\boldsymbol{v}}_h = \int_{\Gamma_{\text{in}}(\hat{K})}\hat{\mathcal{M}}\hat{\boldsymbol{u}}_h^-\cdot\hat{\boldsymbol{v}}_h + h(\hat{f},\hat{\boldsymbol{v}}_h)_{\hat{K}},\end{aligned} \tag{3.4}$$

where quantities marked "ˆ" are defined on $\hat{K}$. By selecting a basis for $\boldsymbol{P}_n(\hat{K})$, (3.4) can be reduced to a linear algebraic system of the form

$$\hat{A}\hat{\boldsymbol{u}} = \hat{\boldsymbol{b}}, \tag{3.5}$$

where

(3.6)
$$\|\hat{\boldsymbol{b}}\|_\infty \le C(|\hat{\boldsymbol{u}}_h^-|_{\infty,\Gamma_{\rm in}(\hat K)} + h\|\hat{\boldsymbol{f}}\|_{\infty,\hat K}) \le C(h^{-N/2}|\boldsymbol{u}_h^-|_{\Gamma_{\rm in}(K)} + h^{(1-N)/2}\|\boldsymbol{f}\|_K),$$
$$\|\boldsymbol{u}_h\|_K \le Ch^{(N+1)/2}\|\hat{\boldsymbol{u}}\|_\infty.$$

If we can show that $\hat A\hat{\boldsymbol{u}} = 0$ has only the trivial solution $\hat{\boldsymbol{u}} \equiv 0$, it will follow that $\boldsymbol{u}_h$ is well defined. This is equivalent to showing that if $\boldsymbol{u}_h^- = 0$ on $\Gamma_{\rm in}(K)$ and $f = 0$ in K, then $\boldsymbol{u}_h = 0$ in K, i.e., if

$$\left((\boldsymbol{u}_h)_t + \sum_{i=1}^N A_i(\boldsymbol{u}_h)_{x_i} + B\boldsymbol{u}_h, \boldsymbol{v}_h\right)_K + \int_{\Gamma_{\rm in}(K)} \mathcal{M}\boldsymbol{u}_h^+ \cdot \boldsymbol{v}_h + \frac{1}{2}\int_{\Gamma^*(K)} (\mathcal{N} - D)\boldsymbol{u}_h \cdot \boldsymbol{v}_h = 0 \qquad \text{all } \boldsymbol{v}_h \in \boldsymbol{P}_n(K), \tag{3.7}$$

then $\boldsymbol{u}_h = 0$ in K. Taking $\boldsymbol{v}_h = \boldsymbol{u}_h$ in (3.7), noting the left side of (3.7) is $a(\boldsymbol{u}_h, \boldsymbol{v}_h)$ (since $\boldsymbol{u}_h^- = 0$ on $\Gamma_{\rm in}(K)$), and applying (3.2), we get

$$\frac{1}{2}\int_{\Gamma_{\rm out}(K)} \mathcal{M}\boldsymbol{u}_h^- \cdot \boldsymbol{u}_h^- + \frac{1}{2}\int_{\Gamma_{\rm in}(K)} \mathcal{M}\boldsymbol{u}_h^+ \cdot \boldsymbol{u}_h^+ + \frac{1}{4}\int_{\Gamma^*(K)} (\mathcal{N} + \mathcal{N}^*)\boldsymbol{u}_h \cdot \boldsymbol{u}_h + \frac{1}{2}\left(\left[B + B^* - \sum_{i=1}^N \frac{\partial A_i}{\partial x_i}\right]\boldsymbol{u}_h, \boldsymbol{u}_h\right)_K = 0.$$

From (1.3), (1.4), and (2.2), we infer that $|\boldsymbol{u}_h^-|_{\Gamma_{\rm out}(K)} = |\boldsymbol{u}_h^+|_{\Gamma_{\rm in}(K)} = 0$.

Now let Γ_k be a face of $\Gamma_{\rm in}(K)$, with unit outer normal $(\boldsymbol{n}_{x,k}, n_{t,k})$, and define

$$\xi_k(\boldsymbol{x}, t) = -\left(\begin{smallmatrix}\boldsymbol{x}-\boldsymbol{x}_k\\ t-t_k\end{smallmatrix}\right)\cdot\left(\begin{smallmatrix}\boldsymbol{n}_{x,k}\\ n_{t,k}\end{smallmatrix}\right),$$

where $(\boldsymbol{x}_k, t_k)$ is an arbitrary point of Γ_k. Note that $|\xi_k(\boldsymbol{x}, t)|$ is the distance from $(\boldsymbol{x}, t)$ to the hyperplane containing Γ_k, and if K is convex, $\xi_k > 0$ in K. Since $\boldsymbol{u}_h^+ = 0$ on $\Gamma_{\rm in}(K)$, $\boldsymbol{u}_h$ in K can be written

$$\boldsymbol{u}_h = \xi_k\boldsymbol{w}_h, \qquad \boldsymbol{w}_h \in \boldsymbol{P}_{n-1}(K), \tag{3.8}$$

where $\xi_k = 0$ on Γ_k and $\boldsymbol{w}_h = 0$ on $\Gamma_{\rm in}(K) \cup \Gamma_{\rm out}(K) - \Gamma_k$. In fact, if $\Gamma_{\rm in}(K) \cup \Gamma_{\rm out}(K)$ consists of m faces, $\boldsymbol{u}_h$ has the representation $\boldsymbol{u}_h = \xi\boldsymbol{w}_h$, where $\xi \in \boldsymbol{P}_m(K), \boldsymbol{w}_h \in \boldsymbol{P}_{n-m}(K)$, and $\xi = 0$ on $\Gamma_{\rm in}(K) \cup \Gamma_{\rm out}(K)$. Thus if $m > n$ (one of the alternatives of assumption (2.3)), then $\boldsymbol{u}_h \equiv 0$ in K.

To complete the proof, we show that the same conclusion holds if K is convex (the other alternative of assumption (2.3)). Applying (3.7) with $\boldsymbol{u}_h = \xi\boldsymbol{w}_h$ (as in (3.8)) and $\boldsymbol{v}_h = \boldsymbol{w}_h$, and using the fact that $\boldsymbol{u}_h^+ = 0$ on $\Gamma_{\rm in}(K)$, we get

$$\Big(\mathcal{L}(\xi_k\boldsymbol{w}_h), \boldsymbol{w}_h\Big)_K + \frac{1}{2}\int_{\Gamma^*(K)} (\mathcal{N} - D)\xi_k\boldsymbol{w}_h \cdot \boldsymbol{w}_h = 0.$$

We have

$$\Big(\mathcal{L}(\xi_k\boldsymbol{w}_h), \boldsymbol{w}_h\Big)_K = \left((\xi_k\boldsymbol{w}_h)_t + \sum_{i=1}^N A_i(\xi_k\boldsymbol{w}_h)_{x_i} + B(\xi_k\boldsymbol{w}_h), \boldsymbol{w}_h\right)_K$$
$$= \left(\left[(\xi_k)_t + \sum_{i=1}^N (\xi_k)_{x_i}A_i + \xi_k B\right]\boldsymbol{w}_h, \boldsymbol{w}_h\right)_K + \left(\xi_k\left[(\boldsymbol{w}_h)_t + \sum_{i=1}^N A_i(\boldsymbol{w}_h)_{x_i}\right], \boldsymbol{w}_h\right)_K$$

and

$$\left(\xi_k\left[(\boldsymbol{w}_h)_t+\sum_{i=1}^N A_i(\boldsymbol{w}_h)_{x_i}\right],\boldsymbol{w}_h\right)_K$$
$$=\frac{1}{2}\left(\xi_k,(|\boldsymbol{w}_h|^2)_t+\sum_{i=1}^N(\boldsymbol{w}_h^TA_i\boldsymbol{w}_h)_{x_i}-\boldsymbol{w}_h^T\sum_{i=1}^N(A_i)_{x_i}\boldsymbol{w}_h\right)_K$$
$$=\frac{1}{2}\oint_{\Gamma(K)}\xi_k\boldsymbol{w}_h^T\left[n_tI+\sum_{i=1}^N n_iA_i\right]\boldsymbol{w}_h$$
$$-\frac{1}{2}\left(\left[(\xi_k)_tI+\sum_{i=1}^N(\xi_k)_{x_i}A_i+\xi_k\sum_{i=1}^N(A_i)_{x_i}\right]\boldsymbol{w}_h,\boldsymbol{w}_h\right)_K.$$

Combining and taking into account the fact that $\xi_k\boldsymbol{w}_h=0$ on $\Gamma_{\text{in}}(K)\cup\Gamma_{\text{out}}(K)$, we get

$$\frac{1}{2}\left(\left\{(\xi_k)_tI+\sum_{i=1}^N(\xi_k)_{x_i}A_i+\xi_k\left[2B-\sum_{i=1}^n(A_i)_{x_i}\right]\right\}\boldsymbol{w}_h,\boldsymbol{w}_h\right)_K+\frac{1}{2}\int_{\Gamma^*(K)}\xi_k\mathcal{N}\boldsymbol{w}_h\cdot\boldsymbol{w}_h=0.$$

Since we are dealing with the case where K is convex, $\xi_k>0$ in K, so

$$\xi_k\left[2B-\sum_{i=1}^N(A_i)_{x_i}\right]\boldsymbol{w}_h\cdot\boldsymbol{w}_h=(\sqrt{\xi_k}\boldsymbol{w}_h)^T\left[B+B^*-\sum_{i=1}^N(A_i)_{x_i}\right]\sqrt{\xi_k}\boldsymbol{w}_h\geq 0.$$

Since from (2.2),

$$(\xi_k)_tI+\sum_{i=1}^N(\xi_k)_{x_i}A_i=-n_{t,k}I-\sum_{i=1}^N n_{x_i,k}A_i=\mathcal{M}|_{\Gamma_k}>0,$$

we obtain

$$\frac{1}{2}\left(\mathcal{M}|_{\Gamma_k}\boldsymbol{w}_h,\boldsymbol{w}_h\right)\leq\frac{1}{2}\left(\left\{(\xi_k)_tI+\sum_{i=1}^N(\xi_k)_{x_i}A_i+\xi_k\left[2B-\sum_{i=1}^n(A_i)_{x_i}\right]\right\}\boldsymbol{w}_h,\boldsymbol{w}_h\right)_K$$
$$+\frac{1}{2}\int_{\Gamma^*(K)}\xi_k\mathcal{N}\boldsymbol{w}_h\cdot\boldsymbol{w}_h=0.$$

Hence, $\boldsymbol{w}_h\equiv 0$, implying $\boldsymbol{u}_h\equiv 0$ in K.

To establish the bound (3.3), we return to (3.5) and write $\hat{A}=\hat{A}_0+\delta\hat{A}$, where $\hat{A}_0$ is the matrix obtained by replacing B with zero and $\hat{A}_1,\ldots,\hat{A}_N$ with their average values over $\hat{K}$. Note that $\hat{A}_0$ is independent of h and that $\|\delta\hat{A}\|\to 0$ as $h\to 0$. We know from the previous uniqueness argument that both $\hat{A}^{-1}$ and $\hat{A}_0^{-1}$ exist. We infer that $\|\hat{A}_0^{-1}\|$ is bounded, independent of h. Moreover, $\|\hat{A}^{-1}\|\to\|\hat{A}_0^{-1}\|$ as $h\to 0$, and $\|\hat{A}^{-1}\|$ is also bounded, independent of h. The desired result (3.3) now follows directly from (3.6). ∎

LEMMA 3.3. *There exist $\gamma>0$, $\mu>0$ such that*

$$\int_{\Gamma_{out}(K)}\mathcal{M}\boldsymbol{u}_h^-\cdot\boldsymbol{u}_h^-+\gamma|[\boldsymbol{u}_h]|^2_{\Gamma_{in}(K)}+\mu\|\boldsymbol{u}_h\|_K^2$$
$$\leq(1+Ch)\int_{\Gamma_{in}(K)}\mathcal{M}\boldsymbol{u}_h^-\cdot\boldsymbol{u}_h^-+C\|\boldsymbol{f}\|_K^2. \tag{3.9}$$

Proof. Taking $\boldsymbol{v}_h = \boldsymbol{u}_h$ in (1.5) and applying (3.2), we obtain

(3.10)
$$\int_{\Gamma(K)-\Gamma^*(K)} \mathcal{M}\boldsymbol{u}_h^- \cdot \boldsymbol{u}_h^- \text{sign}\{n_t\} + \gamma|[\boldsymbol{u}_h]|^2_{\Gamma_{\text{in}}(K)} \le 2(\boldsymbol{f}, \boldsymbol{u}_h)_K \le \|\boldsymbol{u}_h\|^2_K + \|\boldsymbol{f}\|^2_K.$$

Adding to (3.10) a sufficiently large multiple of the square of (3.3) gives (3.9). ∎

To obtain a global stability result, we shall need the following lemma.

LEMMA 3.4. *If* $\{x_i\}$ *satisfies*

$$x_i + a_i \le (1 + \lambda h)x_{i-1} + b_i, \qquad i = 1, 2, \ldots, \tag{3.11}$$

where λ, h, x_0, *and all* a_i*'s and* b_i*'s are nonnegative, then*

$$x_m + \sum_{i=1}^{m} a_i \le e^{\lambda m h}\left(x_0 + \sum_{i=1}^{m} b_i\right).$$

Proof. The solution of 3.11 is

$$\begin{aligned} x_m &\le \sum_{i=1}^{m}(1 + \lambda h)^{m-i}(b_i - a_i) + (1 + \lambda h)^m x_0 \\ &\le (1 + \lambda h)^m \sum_{i=1}^{m} b_i - \sum_{i=1}^{m} a_i + (1 + \lambda h)^m x_0, \end{aligned}$$

and the result follows from the fact that $(1 + \lambda h)^m < e^{\lambda m h}$. ∎

Finally, we combine the previous estimates and use our assumption that there are $O(h^{-1})$ layers in Ω_T to establish the following global stability result.

THEOREM 3.5. *The approximate solution* $\boldsymbol{u}_h$ *satisfies the bound*

$$|\boldsymbol{u}_h^-|^2_{\Gamma_{out}(\Omega_T)} + \|\boldsymbol{u}_h\|^2_{\Omega_T} + \sum_{K\subset\Omega_T} |[\boldsymbol{u}_h]|^2_{\Gamma_{in}(K)} \le C\left(|\boldsymbol{u}_h^-|^2_{\Gamma_{in}(\Omega_T)} + \|\boldsymbol{f}\|^2_{\Omega_T}\right).$$

Proof. Applying (3.9) over a layer of elements S_i (as described in section 2) gives

$$\int_{\mathcal{F}_i} \mathcal{M}\boldsymbol{u}_h^- \cdot \boldsymbol{u}_h^- + \gamma \sum_{K\subset S_i} |[\boldsymbol{u}_h]|^2_{\Gamma_{\text{in}}(K)} + \mu\|\boldsymbol{u}_h\|^2_{S_i} \le (1 + Ch)\int_{\mathcal{F}_{i-1}} \mathcal{M}\boldsymbol{u}_h^- \cdot \boldsymbol{u}_h^- + C\|\boldsymbol{f}\|^2_{S_i}.$$

Application of Lemma 3.4 then yields the desired result. ∎

4. Error estimate. In this section we shall establish the following error estimate between the true solution $\boldsymbol{u}$ and the approximate solution $\boldsymbol{u}_h$.

THEOREM 4.1. *The error* $\boldsymbol{e} \equiv \boldsymbol{u} - \boldsymbol{u}_h$ *satisfies*

$$|\boldsymbol{e}^-|^2_{\Gamma_{out}(\Omega_T)} + \sum_{K\subset\Omega_T} |[\boldsymbol{e}]|^2_{\Gamma_{in}(K)} + \|\boldsymbol{e}\|^2_{\Omega_T} \le Ch^{2n+1}\left(\|\boldsymbol{u}\|^2_{n+1,\Omega_T} + \|\boldsymbol{u}\|^2_{n+1,4,\Omega'_T}\right),$$

where Ω'_T *consists of the union of all elements* K *for which* $\Gamma^*(K)$ *is (a) nonempty and (b) does not lie in a single hyperplane, and* $\|\cdot\|_{m,p,\Omega}$ *denotes the norm in* $W^{m,p}(\Omega)$. *When* $N = 1$, Ω'_T *is empty and the last term on the right may be dropped.*

Proof. Letting $\boldsymbol{u}_I$ denote an appropriate interpolant of $\boldsymbol{u}$, and observing that the exact solution $\boldsymbol{u}$ satisfies

$$a(\boldsymbol{u}, \boldsymbol{v}_h) = (\boldsymbol{f}, \boldsymbol{v}_h)_K \qquad \text{for all } \boldsymbol{v}_h \in \boldsymbol{P}_n(K),$$

we easily obtain the error equation

$$a(\boldsymbol{e}_h, \boldsymbol{v}_h) = a(\boldsymbol{e}_I, \boldsymbol{v}_h) \qquad \text{for all } \boldsymbol{v}_h \in \boldsymbol{P}_n(K), \tag{4.1}$$

where $\boldsymbol{e}_h = \boldsymbol{u}_h - \boldsymbol{u}_I$ and $\boldsymbol{e}_I = \boldsymbol{u} - \boldsymbol{u}_I$. First consider the test function $\boldsymbol{v}_h = \boldsymbol{e}_h$. Using (3.2), we have

(4.2)
$$a(\boldsymbol{e}_h, \boldsymbol{e}_h) = a(\boldsymbol{e}_I, \boldsymbol{e}_h) = (\boldsymbol{e}_I, \mathcal{L}^* \boldsymbol{e}_h)_K - \int_{\Gamma_{\text{in}}(K)} [\mathcal{M}\boldsymbol{e}_h] \cdot \boldsymbol{e}_I - \frac{1}{2} \int_{\Gamma^*(K)} (\mathcal{N} - D)\boldsymbol{e}_h \cdot \boldsymbol{e}_I$$
$$+ \int_{\Gamma(K) - \Gamma^*(K)} \mathcal{M}\boldsymbol{e}_I^- \cdot \boldsymbol{e}_h^- \text{sign}\{n_t\} + \int_{\Gamma_{\text{in}}(K)} \mathcal{M}[\boldsymbol{e}_I] \cdot [\boldsymbol{e}_h] + \frac{1}{2} \int_{\Gamma^*(K)} (\mathcal{N} + \mathcal{N}^*)\boldsymbol{e}_I \cdot \boldsymbol{e}_h.$$

We now define a specific interpolant $\boldsymbol{u}_I$. To do this, we must distinguish three possibilities for $\Gamma^*(K)$. The first case is when $\Gamma^*(K)$ is empty: here we define $\boldsymbol{u}_I$ to be the $L^2(K)$ projection of $\boldsymbol{u}$ onto $\boldsymbol{P}_n(K)$. In the second case, where $\Gamma^*(K)$ lies in a single hyperplane (this occurs only at boundary vertices), we define $\boldsymbol{u}_I$ by the conditions:

$$(\boldsymbol{u} - \boldsymbol{u}_I, \boldsymbol{v}_h)_K = 0 \qquad \text{for all } \boldsymbol{v}_h \in \boldsymbol{P}_{n-1}(K),$$
$$\int_{\Gamma^*(K)} (\boldsymbol{u} - \boldsymbol{u}_I) \cdot \boldsymbol{v}_h = 0 \qquad \text{for all } \boldsymbol{v}_h \in \boldsymbol{P}_n(\Gamma^*(K)).$$

It is not difficult to check that this is an optimal order interpolant. Finally, there is the remaining case in which $\Gamma^*(K)$ is contained by more than one hyperplane, which occurs at boundary vertices where the normal to Ω_T is not constant. In this case, we again define $\boldsymbol{u}_I$ to be the $L^2(K)$ projection of $\boldsymbol{u}$ onto $\boldsymbol{P}_n(K)$. When Ω is an interval in $\mathbb{R}^1$, only the first two cases arise and the second case arises only at each of the two endpoints of Ω, where $\Gamma^*(K)$ consists of a single edge. If Ω is a polygon in $\mathbb{R}^2$, then case 2 arises at mesh vertices which lie on $\partial\Omega$, except at the corners of the polygon. Case 3 occurs at precisely the corners of the polygon. It is case 3 which causes some extra technicalities in the analysis below.

We denote by $\mathcal{L}_0^*$ the operator obtained by replacing the coefficients A_i and B in $\mathcal{L}^*$ by their average values on each element K, and by $\mathcal{N}_0$ and D_0 the operators obtained by replacing $\mathcal{N}$ and D, respectively, by their average values over $\Gamma^*(K)$. Via standard inverse inequalities and approximation results, we obtain

$$|(\boldsymbol{e}_I, \mathcal{L}^* \boldsymbol{e}_h)_K| \le |(\boldsymbol{e}_I, \mathcal{L}_0^* \boldsymbol{e}_h)_K| + |(\boldsymbol{e}_I, \mathcal{L}^* \boldsymbol{e}_h - \mathcal{L}_0^* \boldsymbol{e}_h)_K| \le C \|\boldsymbol{e}_I\|_K \|\boldsymbol{e}_h\|_K$$

for all K. In case 2 ($\Gamma^*(K)$ lying in a single hyperplane), we obtain

$$\left| \int_{\Gamma^*(K)} (\mathcal{N} - D)\boldsymbol{e}_h \cdot \boldsymbol{e}_I \right| \le \left| \int_{\Gamma^*(K)} (\mathcal{N}_0 - D_0)\boldsymbol{e}_h \cdot \boldsymbol{e}_I \right| + \left| \int_{\Gamma^*(K)} (\mathcal{N} - \mathcal{N}_0 - D + D_0)\boldsymbol{e}_h \cdot \boldsymbol{e}_I \right|$$
$$\le Ch |\boldsymbol{e}_h|_{\Gamma^*(K)} |\boldsymbol{e}_I|_{\Gamma^*(K)} \le Ch^{1/2} \|\boldsymbol{e}_h\|_K |\boldsymbol{e}_I|_{\Gamma^*(K)},$$

and, in case 3 ($\Gamma^*(K)$ not lying in a single hyperplane),

$$\left| \int_{\Gamma^*(K)} (\mathcal{N} - D)\boldsymbol{e}_h \cdot \boldsymbol{e}_I \right| \le C |\boldsymbol{e}_h|_{\Gamma^*(K)} |\boldsymbol{e}_I|_{\Gamma^*(K)} \le Ch^{-1/2} \|\boldsymbol{e}_h\|_K |\boldsymbol{e}_I|_{\Gamma^*(K)}.$$

Hence, using (4.2) and (3.2), we get that

$$\frac{1}{2}\int_{\Gamma(K)-\Gamma^*(K)} \mathcal{M}\boldsymbol{e}_h^- \cdot \boldsymbol{e}_h^- \operatorname{sign}\{n_t\} + \frac{\gamma}{2}|[\boldsymbol{e}_h]|^2_{\Gamma_{\rm in}(K)} + \frac{1}{4}\int_{\Gamma^*(K)} (\mathcal{N}+\mathcal{N}^*)\boldsymbol{e}_h \cdot \boldsymbol{e}_h$$
$$\le C\left(|[\boldsymbol{e}_h]|_{\Gamma_{\rm in}(K)}|\boldsymbol{e}_I^-|_{\Gamma_{\rm in}(K)} + |[\boldsymbol{e}_h]|_{\Gamma_{\rm in}(K)}|[\boldsymbol{e}_I]|_{\Gamma_{\rm in}(K)} + h^\alpha \|\boldsymbol{e}_h\|_K |\boldsymbol{e}_I|_{\Gamma^*(K)}\right)$$
$$+\int_{\Gamma(K)-\Gamma^*(K)} \mathcal{M}\boldsymbol{e}_I^- \cdot \boldsymbol{e}_h^- \operatorname{sign}\{n_t\} + \frac{1}{2}\left[\int_{\Gamma^*(K)} (\mathcal{N}+\mathcal{N}^*)\boldsymbol{e}_I \cdot \boldsymbol{e}_I\right]^{1/2}\left[\int_{\Gamma^*(K)} (\mathcal{N}+\mathcal{N}^*)\boldsymbol{e}_h \cdot \boldsymbol{e}_h\right]^{1/2},$$

where $\alpha = 1/2$ when $\Gamma^*(K)$ lies in a single hyperplane, $\alpha = -1/2$ when $\Gamma^*(K)$ does not lie in a single hyperplane, and the term involving h^α is omitted when $\Gamma^*(K)$ is empty. After applying the arithmetic-geometric mean inequality, we obtain

$$\frac{1}{2}\int_{\Gamma(K)-\Gamma^*(K)} \mathcal{M}\boldsymbol{e}_h^- \cdot \boldsymbol{e}_h^- \operatorname{sign}\{n_t\} + \frac{\tilde\gamma}{2}|[\boldsymbol{e}_h]|^2_{\Gamma_{\rm in}(K)} \le \int_{\Gamma(K)-\Gamma^*(K)} \mathcal{M}\boldsymbol{e}_I^- \cdot \boldsymbol{e}_h^- \operatorname{sign}\{n_t\}$$
$$+ \|\boldsymbol{e}_h\|_K^2 + C\left(|\boldsymbol{e}_I^-|^2_{\Gamma_{\rm in}(K)} + |[\boldsymbol{e}_I]|^2_{\Gamma_{\rm in}(K)} + (1+h^{2\alpha})|\boldsymbol{e}_I|^2_{\Gamma^*(K)}\right).$$

We complete the square on the $\Gamma(K)-\Gamma^*(K)$ integrals, write $\boldsymbol{e}_h = \boldsymbol{e}_I - \boldsymbol{e}$, and make repeated use of the Schwarz inequality to obtain

$$\frac{1}{2}\int_{\Gamma(K)-\Gamma^*(K)} \mathcal{M}\boldsymbol{e}^- \cdot \boldsymbol{e}^- \operatorname{sign}\{n_t\} + \frac{\tilde\gamma}{2}|[\boldsymbol{e}]|^2_{\Gamma_{\rm in}(K)} \le 2\|\boldsymbol{e}\|_K^2 + CR_K(\boldsymbol{e}_I),$$

where

$$R_K(\boldsymbol{e}_I) \equiv |\boldsymbol{e}_I^-|^2_{\Gamma_{\rm in}(K)} + |\boldsymbol{e}_I^-|^2_{\Gamma_{\rm out}(K)} + |[\boldsymbol{e}_I]|^2_{\Gamma_{\rm in}(K)} + (1+h^{2\alpha})|\boldsymbol{e}_I|^2_{\Gamma^*(K)}.$$

Using standard results from approximation theory, it easily follows that

$$R_K(\boldsymbol{e}_I) \le Ch^{2n+1+\min(0,2\alpha)}\|\boldsymbol{u}\|^2_{n+1,K}.$$

Thus

$$\int_{\Gamma_{\rm out}(K)} \mathcal{M}\boldsymbol{e}^- \cdot \boldsymbol{e}^- + \tilde\gamma|[\boldsymbol{e}]|^2_{\Gamma_{\rm in}(K)} \tag{4.3}$$
$$\le \int_{\Gamma_{\rm in}(K)} \mathcal{M}\boldsymbol{e}^- \cdot \boldsymbol{e}^- + 4\|\boldsymbol{e}\|_K^2 + Ch^{2n+1+\min(0,2\alpha)}\|u\|^2_{n+1,K}.$$

To gain control of $\boldsymbol{e}$ inside element K, we write (4.1) as

$$a(\boldsymbol{e}_h, \boldsymbol{v}_h) = (F, \boldsymbol{v}_h)_K,$$

where F is defined through the inner product conditions:

$$(F, \boldsymbol{v}_h)_K = a(\boldsymbol{e}_I, \boldsymbol{v}_h) = (\mathcal{L}\boldsymbol{e}_I, \boldsymbol{v}_h)_K + \int_{\Gamma_{\rm in}(K)} \mathcal{M}[\boldsymbol{e}_I]\cdot \boldsymbol{v}_h + \frac{1}{2}\int_{\Gamma^*(K)} (\mathcal{N}-D)\boldsymbol{e}_I \cdot \boldsymbol{v}_h.$$

Using standard results from approximation theory,

$$|(F, \boldsymbol{v}_h)_K| \le Ch^n\|\boldsymbol{u}\|_{n+1,K}\|\boldsymbol{v}_h\|_K,$$

which implies

$$\|F\|_K \le Ch^n\|\boldsymbol{u}\|_{n+1,K}.$$

Applying (3.3), we get

$$\|\boldsymbol{e}_h\|_K \le C(\sqrt{h}|\boldsymbol{e}_h^-|_{\Gamma_{\rm in}(K)} + h^{n+1}\|\boldsymbol{u}\|_{n+1,K}).$$

Replacing $\boldsymbol{e}_h$ by $\boldsymbol{e}_I - \boldsymbol{e}$ leads to

$$\|\boldsymbol{e}\|_K \le C(\sqrt{h}|\boldsymbol{e}^-|_{\Gamma_{\rm in}(K)} + h^{n+1}\|\boldsymbol{u}\|_{n+1,K}). \tag{4.4}$$

We now add 5 times the square of (4.4) to (4.3) to obtain

$$\begin{aligned}\int_{\Gamma_{\rm out}(K)} \mathcal{M}\boldsymbol{e}^-\cdot\boldsymbol{e}^- + \tilde{\gamma}|[\boldsymbol{e}]|^2_{\Gamma_{\rm in}(K)} + \|\boldsymbol{e}\|^2_K \\ \le (1+Ch)\int_{\Gamma_{\rm in}(K)} \mathcal{M}\boldsymbol{e}^-\cdot\boldsymbol{e}^- + Ch^{2n+1+\min(0,2\alpha)}\|\boldsymbol{u}\|^2_{n+1,K}.\end{aligned} \tag{4.5}$$

Applying this over a layer of elements S_i gives

$$\begin{aligned}\int_{\mathcal{F}_i} \mathcal{M}\boldsymbol{e}^-\cdot\boldsymbol{e}^- + \tilde{\gamma}\sum_{K\subset S_i}|[\boldsymbol{e}]|^2_{\Gamma_{\rm in}(K)} + \|\boldsymbol{e}\|^2_{S_i} \\ \le (1+Ch)\int_{\mathcal{F}_{i-1}} \mathcal{M}\boldsymbol{e}^-\cdot\boldsymbol{e}^- + Ch^{2n+1}\|\boldsymbol{u}\|^2_{n+1,S_i} + Ch^{2n}\|\boldsymbol{u}\|^2_{n+1,S_i'},\end{aligned} \tag{4.6}$$

where S_i' denotes the set of elements in S_i for which $\alpha = -1/2$. Application of Lemma 3.4 yields

$$|\boldsymbol{e}^-|^2_{\Gamma_{\rm out}(\Omega_T)} + \sum_{K\subset\Omega_T}|[\boldsymbol{e}]|^2_{\Gamma_{\rm in}(K)} + \|\boldsymbol{e}\|^2_{\Omega_T} \le Ch^{2n+1}\|\boldsymbol{u}\|^2_{n+1,\Omega_T} + Ch^{2n}\|\boldsymbol{u}\|^2_{n+1,\Omega_T'}.$$

Since $\mathrm{meas}(\Omega_T') \le Ch^2$,

$$\|D^\alpha\boldsymbol{u}\|^2_{\Omega_T'} = \int_{\Omega_T'}|D^\alpha\boldsymbol{u}|^2 \le \mathrm{meas}(\Omega_T')^{1/2}\left(\int_{\Omega_T'}|D^\alpha\boldsymbol{u}|^4\right)^{1/2} \le Ch\|D^\alpha\boldsymbol{u}\|^2_{0,4,\Omega_T'}.$$

Hence,

$$\begin{aligned}\|\boldsymbol{u}\|^2_{n+1,\Omega_T'} = \sum_{|\alpha|\le n+1}\|D^\alpha\boldsymbol{u}\|^2_{\Omega_T'} \le Ch\sum_{|\alpha|\le n+1}\|D^\alpha\boldsymbol{u}\|^2_{0,4,\Omega_T'} \\ \le Ch\left(\sum_{|\alpha|\le n+1}1^2\right)^{1/2}\left(\sum_{|\alpha|\le n+1}\|D^\alpha\boldsymbol{u}\|^4_{0,4,\Omega_T'}\right)^{1/2} \le Ch\|\boldsymbol{u}\|^2_{n+1,4,\Omega_T'}.\end{aligned} \tag{4.7}$$

The desired result follows immediately from this estimate. ∎

5. A numerical example. In this section, we present the results of some numerical computations. We use as our test problem the wave equation in two space dimensions, written as a first order system as in section 1. We take Ω to be the square $0 < x < 2\pi$, $0 < y < 2\pi$ and impose periodic boundary conditions. At $t = 0$ we take

$$u_1 = u_2 = 0, \quad u_3 = \sqrt{2}\sin x \sin y.$$

TABLE 5.1

N	$\lvert\boldsymbol{u}_h - \boldsymbol{u}\rvert_{t=1}$	$\lvert\boldsymbol{u}_h - \boldsymbol{u}\rvert_{t=2}$
6	.270	.438
12	.951(-1) [2.89]	.150 [2.92]
24	.202(-1) [4.71]	.289(-1) [5.19]
48	.440(-2) [4.51]	.527(-2) [5.48]
96	.104(-2) [4.23]	.112(-2) [4.71]
192	.257(-3) [4.05]	.266(-3) [4.21]
384	.640(-4) [4.02]	.655(-4) [4.06]

The exact solution for $t > 0$ is then

$$u_1 = \cos x \sin y \sin \sqrt{2}t, \qquad u_2 = \sin x \cos y \sin \sqrt{2}t, \qquad u_3 = \sqrt{2} \sin x \sin y \cos \sqrt{2}t.$$

Our space-time mesh is based on a regular subdivision of Ω into right isosceles triangles, as shown in Figure 2.8. Each space-time element is a union of six tetrahedra, analogous to those described in the text accompanying Figure 2.8. The condition for "explicitness" of this mesh for the wave equation is $\Delta t/h \leq .707$. In our numerical experiments, we use linear approximation with $\Delta t/h = .637$. In Table 5.1, L^2 errors in $\boldsymbol{u}_h$ are given at $t = 1$ and $t = 2$ vs. N, the number of subintervals into which $[0, 2\pi]$ is divided. These results indicate an optimal $O(h^2)$ rate of convergence, in contrast to our theoretical estimate of $O(h^{1.5})$. This $h^{1/2}$ gap between theoretical and actual convergence rates is typical for the discontinuous Galerkin method (cf. [10] and [11]).

REFERENCES

[1] Q. Du, M. Gunzburger, and W. Layton, *A low dispersion, high accuracy finite element method for first order hyperbolic systems in several space variables. Hyperbolic partial differential equations.* V, Comput. Math. Appl., 15 (1988), pp. 447–457.

[2] K. O. Friedrichs, *Symmetric positive linear differential equations*, Comm. Pure Appl. Math., 11 (1958), pp. 333–418.

[3] M. Gunzburger, *On the stability of Galerkin methods for initial-boundary value problems for hyperbolic systems*, Math. Comp., 31 (1977), pp. 661–675.

[4] C. Johnson, U. Nävert, and J. Pitkäranta, *Finite element methods for linear hyperbolic problems*, Comput. Methods Appl. Mech. Engrg., 45 (1984), pp. 285–312.

[5] C. Johnson and J. Pitkäranta, *An analysis of the discontinuous Galerkin method for a scalar hyperbolic equation*, Math. Comp., 46 (1986), pp. 1–26.

[6] W. Layton, *Stable Galerkin methods for hyperbolic systems*, SIAM J. Numer. Anal., 20 (1983), pp. 221–233.

[7] W. Layton, *High-accuracy finite-element methods for positive symmetric systems. Hyperbolic partial differential equations.* III, Comput. Math. Appl. Part A, 12 (1986), pp. 565–579.

[8] P. Lesaint, *Finite element methods for symmetric hyperbolic equations*, Numer. Math., 21 (1973), pp. 244–255.

[9] P. Lesaint and P. A. Raviart, *On a finite element method for solving the neutron transport equation*, in Mathematical Aspects of Finite Elements in Partial Differential Equations, C. deBoor, ed., Academic Press, New York, 1974, pp. 89–123.

[10] T. E. Peterson, *A note on the convergence of the discontinuous Galerkin method for a scalar hyperbolic equation*, SIAM J. Numer. Anal., 28 (1991), pp. 133–140.

[11] G. R. Richter, *An optimal-order error estimate for the discontinuous Galerkin method*, Math. Comp., 50 (1988), pp. 75–88.

[12] G. Richter, *An explicit finite element method for the wave equation*, Appl. Numer. Math., 16 (1994), pp. 65–80.

[13] R. Winther, *A stable finite element method for first-order hyperbolic systems*, Math. Comp., 36 (1981), pp. 65–86.